
This copy is for your personal, non-commercial use only.

If you wish to distribute this article to others, you can order high-quality copies for your colleagues, clients, or customers by [clicking here](#).

Permission to republish or repurpose articles or portions of articles can be obtained by following the guidelines [here](#).

The following resources related to this article are available online at www.sciencemag.org (this information is current as of August 30, 2011):

Updated information and services, including high-resolution figures, can be found in the online version of this article at:

<http://www.sciencemag.org/content/292/5522/1722.full.html>

Supporting Online Material can be found at:

<http://www.sciencemag.org/content/suppl/2003/01/09/292.5522.1722.DC1.html>

A list of selected additional articles on the Science Web sites **related to this article** can be found at:

<http://www.sciencemag.org/content/292/5522/1722.full.html#related>

This article **cites 22 articles**, 5 of which can be accessed free:

<http://www.sciencemag.org/content/292/5522/1722.full.html#ref-list-1>

This article has been **cited by** 231 article(s) on the ISI Web of Science

This article has been **cited by** 97 articles hosted by HighWire Press; see:

<http://www.sciencemag.org/content/292/5522/1722.full.html#related-urls>

This article appears in the following **subject collections**:

Microbiology

<http://www.sciencemag.org/cgi/collection/microbio>

and cultured to stage 10 (2 to 3 hours). Twenty explants were processed in each sample and the presence of mRNA encoding the Wnt-responsive genes *Siamois* and *Xnr-3* and control (Histone H4 and translational elongation factor 1 α , *EF-1 α*) was detected by RT-PCR analysis at the 16-cell stage, as described elsewhere (3).

24. C. C. Malbon *et al.*, unpublished data.
 25. R. T. Moon *et al.*, *Development* **119**, 97 (1993).
 26. J. L. Christian, J. A. McMahon, A. P. McMahon, R. T. Moon, *Development* **111**, 1045 (1991).
 27. S. D. Chan *et al.*, *J. Biol. Chem.* **267**, 25202 (1992).
 28. C. C. Malbon, *J. Biol. Chem.* **255**, 8692 (1980).

29. M. Ros, J. K. Northup, C. C. Malbon, *J. Biol. Chem.* **263**, 4362 (1988).
 30. Supported by grants from NIH. R.T.M. is an investigator of the Howard Hughes Medical Institute.

22 February 2001; accepted 23 April 2001

A Transgenic Model for Listeriosis: Role of Internalin in Crossing the Intestinal Barrier

Marc Lecuit,¹ Sandrine Vandormael-Pournin,² Jean Lefort,³ Michel Huerre,⁴ Pierre Gounon,⁵ Catherine Dupuy,¹ Charles Babinet,² Pascale Cossart^{1*}

Listeria monocytogenes is responsible for severe food-borne infections, but the mechanisms by which bacteria cross the intestinal barrier are unknown. *Listeria monocytogenes* expresses a surface protein, internalin, that interacts with a host receptor, E-cadherin, to promote entry into human epithelial cells. Murine E-cadherin, in contrast to guinea pig E-cadherin, does not interact with internalin, excluding the mouse as a model for addressing internalin function in vivo. In guinea pigs and transgenic mice expressing human E-cadherin, internalin was found to mediate invasion of enterocytes and crossing of the intestinal barrier. These results illustrate how relevant animal models for human infections can be generated.

Understanding how bacteria cross the intestinal barrier is a key issue in the study of foodborne diseases. *Listeria monocytogenes* causes listeriosis, an infection characterized by bacterial dissemination from the intestinal lumen to the central nervous system and the fetoplacental unit (1). As recently shown, *L. monocytogenes* is also responsible for gastroenteritis (2, 3). How this bacterium crosses the intestinal barrier is unknown. In vitro, the *L. monocytogenes* surface protein internalin promotes bacterial internalization into human epithelial cells (4). Its receptor is E-cadherin (5), a protein that mediates the formation of adherens junctions between epithelial cells and is also expressed on the basolateral face of polarized epithelial cells (6). In contrast to human E-cadherin (hEcad), mouse and rat E-cadherins are not receptors for internalin, and internalin plays no role in entry into mouse and rat epithelial cells (7). We have shown that this specificity relies on the nature of the sixteenth amino acid, a proline in hEcad, and a glutamic acid in mouse and rat E-cadherins (7). We concluded that although rat and mouse can be successfully used to study the T cell response to intravenous (IV) infection of *L. monocytogenes*, they are inappropriate models for studying internalin func-

tion in vivo. In mice, oral infections are not reproducibly lethal, and bacterial translocation across the intestinal barrier is low. More-

over, in these animals, specific targeting to the brainstem and the fetoplacental unit is not seen, even after IV inoculation.

Guided by the pioneering work of Racz *et al.* (8), we observed that a guinea pig epithelial cell line allows entry of *L. monocytogenes* strain EGD at an efficiency 200 times that of isogenic internalin deletion mutant EGD Δ inlA (7). These results correlated with the finding that guinea pig E-cadherin harbors a proline at position 16 and led us to propose that the role of internalin in vivo could be addressed with guinea pigs or transgenic mice expressing hEcad. We report the results of oral infections of both guinea pigs and transgenic mice expressing hEcad on their enterocytes and show that internalin is a virulence factor mediating crossing of the intestinal barrier.

IV infections of mice with *L. monocytogenes* are lethal. The median lethal dose (LD₅₀) of EGD or EGD Δ inlA is similar (~10⁵ bacteria) (9). In contrast, oral infections with even 5 × 10¹⁰ EGD or EGD Δ inlA

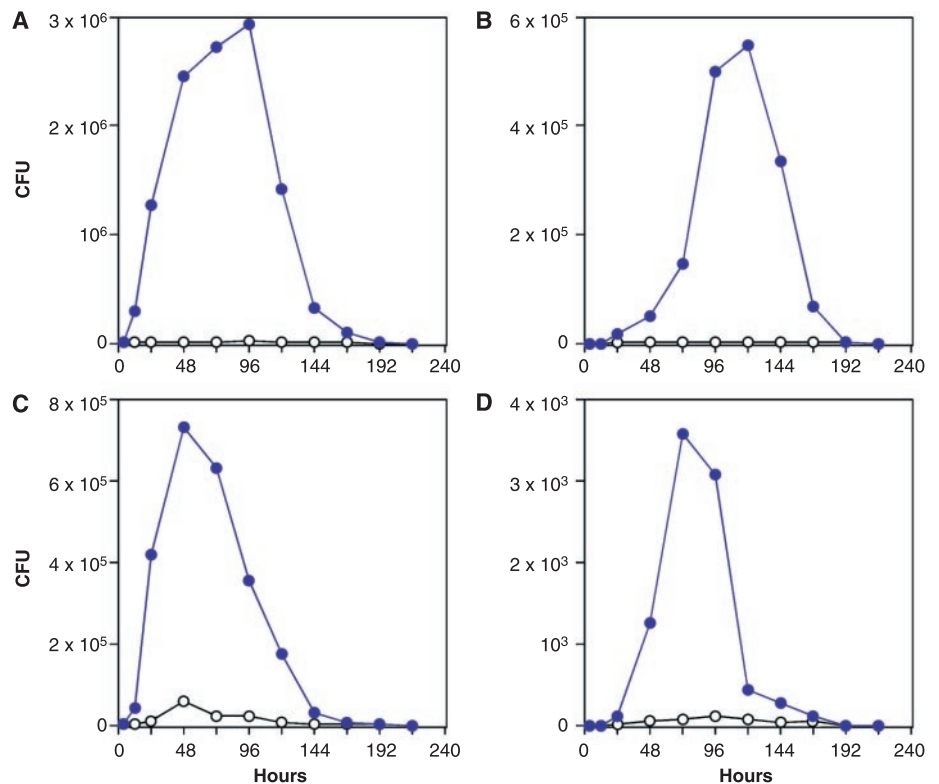


Fig. 1. Role of internalin in the bacterial invasion of guinea pig (A) small intestine, (B) liver, (C) mesenteric lymph nodes, and (D) spleen. Bacterial counts in organs of guinea pigs infected orally with 10¹⁰ *L. monocytogenes* wild-type strain EGD (purple plots) and the internalin deletion mutant EGD Δ inlA (white plots) are shown (9). Mean colony-forming units (CFU) from four different animals are given at each time point.

¹Unité des Interactions Bactéries-Cellules, ²Unité de Biologie du Développement, Unité de Recherche Associée CNRS 1960, ³Unité de Pharmacologie Cellulaire, ⁴Unité d'Histopathologie, ⁵Station Centrale de Microscopie Electronique, Institut Pasteur, 75724 Paris cedex 15, France.

*To whom correspondence should be addressed. E-mail: pcossart@pasteur.fr

REPORTS

are not lethal, and few bacteria cross the intestinal barrier (7, 9). We infected guinea pigs to assess *L. monocytogenes* virulence via the oral route in a model in which the role of internalin could be tested. Oral infection with 5×10^{11} EGD resulted in 100% mortality, and infection with 10^{10} EGD resulted in 100% survival; the LD₅₀ is 10^{11} bacteria (Web fig. 1) (9). In contrast, infection with 5×10^{11} EGD Δ *inlA* resulted in 100% survival. Thus, internalin acts as a virulence factor in guinea pigs. Because E-cadherin is expressed in various epithelial cells, internalin may be critical after crossing of the intestinal barrier at a later stage of infection. We thus tested the role of internalin after an IV infection (9). The LD₅₀ values of EGD and EGD Δ *inlA* after IV infection of guinea pigs were identical ($\sim 5 \times 10^7$ bacteria), and the number of bacteria present in the liver and spleen 72 hours after IV inoculation with 10^6 EGD or EGD Δ *inlA* is similar (9, 10). The absence of a detectable role for internalin in infections initiated via the IV route, together with internalin-dependent mortality after oral infection, suggested a critical role for internalin at an early stage of infection, between bacterial ingestion and access to the bloodstream. We followed bacterial invasion in the small intestine of guinea pigs and translocation into the mesenteric lymph nodes, liver, and spleen using different inocula (5×10^{11} , 10^{11} , and 10^{10} bacteria). Wild-type bacteria

invade the intestinal tissue and reach deeper organs, whereas EGD Δ *inlA* bacteria do not (Fig. 1). This process is dose dependent (10) and internalin dependent (Fig. 1). Intestinal invasion is not promoted by the presence of Peyer's patches, as the ratio of bacterial counts of EGD versus EGD Δ *inlA* is more than one order of magnitude higher in intestinal portions without Peyer's patches than in isolated Peyer's patches (Web fig. 2) (9). Intestinal sections immunolabeled with antibody to *L. monocytogenes* and electron microscopy revealed the presence of intraenterocytic *L. monocytogenes* 12 hours after bacterial ingestion (Fig. 2). Despite extensive searching, EGD Δ *inlA* was not detected within enterocytes. To verify these findings, we used *L. innocua*, a nonpathogenic species that becomes invasive when transformed with *inlA*. Ex vivo infection of intestinal samples with *L. innocua* (*inlA*), in contrast to wild-type *L. innocua*, resulted in the invasion of enterocytes, confirming that internalin was able to mediate invasion of those cells (Web fig. 3) (9).

In animals infected orally with wild-type *L. monocytogenes*, intravillous abscesses, i.e., foci of bacterial multiplication and recruitment of polymorphonuclear cells and monocytes, were detected as early as 12 hours after bacterial ingestion. Their size and number correlated with bacterial counts and reached a maximum 72 to 120 hours after infection

(Figs. 1 and 2A). In animals infected with high doses of EGD Δ *inlA* (5×10^{11} bacteria), bacteria were occasionally seen in the intestine, either in Peyer's patches or in regions where the epithelial monolayer was damaged, but intravillous abscesses similar to those observed with EGD were not seen with EGD Δ *inlA*.

To demonstrate and elucidate the role of the internalin E-cadherin interaction in vivo, we generated transgenic mice that express hEcad solely in enterocytes. This was achieved by placing the hEcad gene under the control of the *iFABP* promoter (9, 11). *iFABP* encodes the intestinal isoform of the fatty acid binding protein whose expression is restricted to epithelial cells of the small intestine (12). Several transgenic founders were obtained, and the corresponding lines were established and tested (9, 11). One of them, exhibiting the expected hEcad expression pattern, i.e., restricted to enterocytes, was further characterized (Web fig. 4) (9). Parental and transgenic intestinal morphologies were indistinguishable (10). Oral infections of nontransgenic mice with 5×10^{10} wild-type bacteria or the internalin mutant resulted in complete survival of the animals (Fig. 3A). In contrast, infection of transgenic mice resulted in $\sim 85\%$ mortality with this infective dose of wild-type bacteria and zero mortality with the same dose of the internalin mutant (Fig. 3A). Moreover, a kinetic analysis of

Fig. 2. Internalin-mediated invasion of enterocytes and crossing of the intestinal barrier in guinea pigs. (A) Histological sections of intestinal samples after oral infection of guinea pigs with wild-type (WT) *L. monocytogenes* (left) and the internalin mutant Δ *inlA* (right). Arrows show bacteria, which appear red; scale bars, 10 μ m (9). (B) Thin sections of an intestinal sample from guinea pig infected with wild-type *L. monocytogenes*. Intestinal portions were dissected and fixed 12 hours after infection (5, 9). The bottom panels show enlargements of three intraenterocytic *L. monocytogenes* in the top panel: one is still in a phagocytic vacuole (left); one is partially surrounded with actin in a two-membrane vacuole, suggesting that it had spread from one cell to the next (middle); and one is dividing in the cytosol (right).

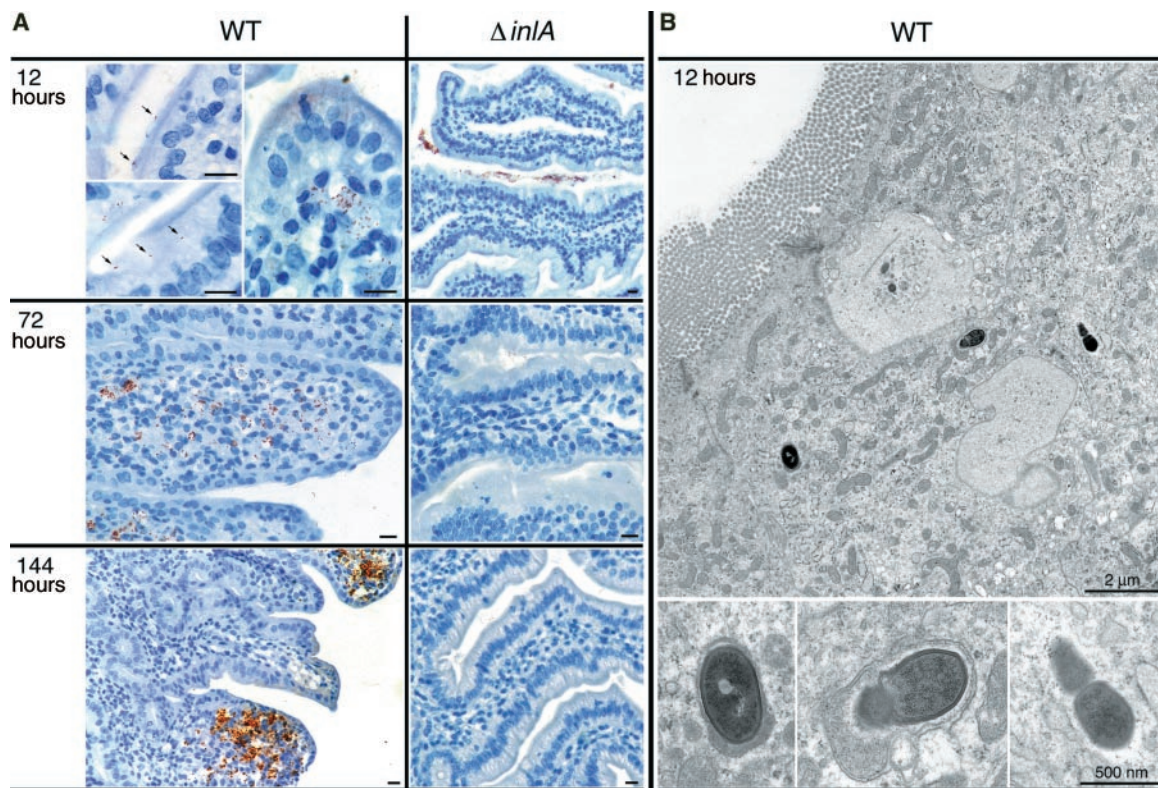
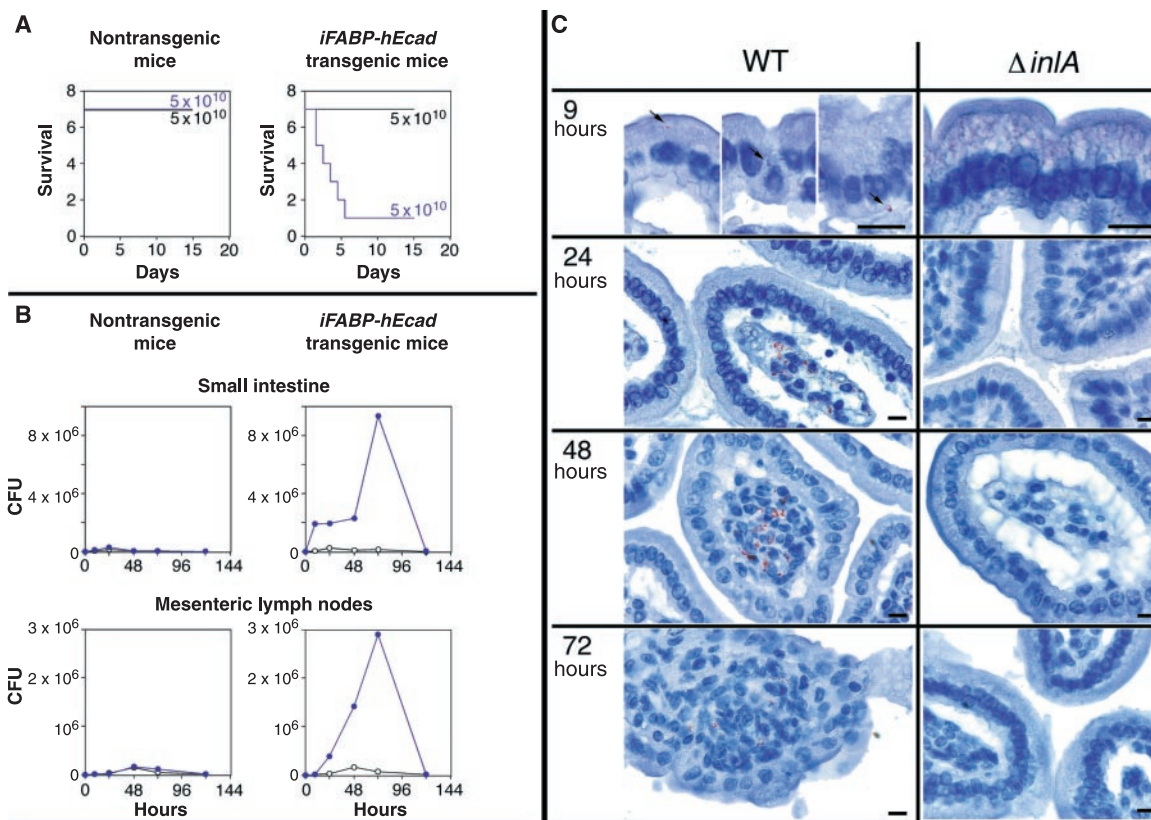


Fig. 3. Infection of transgenic mice expressing hEcad on their enterocytes by *L. monocytogenes* and the internalin deletion mutant. **(A)** Survival of nontransgenic mice and *iFABP-hEcad* transgenic mice after oral infection with 5×10^{10} wild-type (WT) *L. monocytogenes* (purple plots) and the internalin mutant Δ *inIA* (black plots) (9). **(B)** Bacterial counts in organs of nontransgenic mice (left) or *iFABP-hEcad* transgenic mice (right) infected with 10^{10} wild-type *L. monocytogenes* (purple plots) and the internalin mutant Δ *inIA* (white plots) (mean CFU from three animals for each time point) (9). **(C)** Histological sections of intestinal samples after oral infection of *iFABP-hEcad* transgenic mice with wild-type *L. monocytogenes* (left) and the internalin mutant Δ *inIA* (right) (scale bars, 10 μ m) (9).



bacterial counts in intestine and mesenteric lymph nodes (Fig. 3B) and immunohistochemical studies (Fig. 3C) showed that the internalin hEcad interaction mediated invasion of enterocytes and subsequent intravillous bacterial multiplication, abscess formation, and access to mesenteric lymph nodes, liver, and spleen (10).

In conclusion, these data establish that interaction of internalin with E-cadherin on enterocytes is an early critical step for the onset of listeriosis in vivo. From data obtained in the mouse and rat species, the intestinal phase of human listeriosis was previously assumed to be almost silent and intestinal translocation of bacteria was assumed to be a nonspecific event (13). Listeriosis was thought to be mainly due to the ability of *L. monocytogenes* to survive inside phagocytic cells of deeper tissues once across the epithelial barrier. But as reported recently (2, 3), ingestion of large numbers of *L. monocytogenes* (up to 3×10^{11} bacteria per individual) is associated with gastroenteritis. Our results confirmed this enteropathogenicity and offer a molecular basis for this observation. In addition, by promoting invasion of enterocytes and translocation across the intestinal barrier, internalin also mediates access to deeper tissues and should now be considered a virulence factor as important as other well-characterized virulence factors, such as listeriolysin O and ActA (14).

E-cadherin is mostly expressed at adherens junctions of enterocytes (6) and does not appear to be accessible from the apical side of enterocytes in the intestinal brush border. How does internalin reach E-cadherin? The intestinal mucosa is a fast renewing tissue (12). Enterocytes, at the tip of villi, are replaced by ascending enterocytes produced in intestinal crypts, and the transient opening of cell-cell junctions between enterocytes may allow E-cadherin to interact with bacteria (12, 15). Consistent with this hypothesis, *L. monocytogenes* was more frequently found at the tip of intestinal villi in guinea pigs and transgenic mice. Yet, invasion of enterocytes in vivo remains a rare event, as abscesses were not detected in all villi, although each intestinal villus possesses thousands of cells.

InIB, another invasion surface protein of *L. monocytogenes* that mediates entry into various cell types in vitro (16), might promote internalin access to E-cadherin in vivo. Indeed, InIB has been shown to interact with Met, the hepatocyte growth factor receptor, which is also expressed on enterocytes and whose activation can result in disruption of cell-cell junctions (17, 18). *Listeria monocytogenes* may also enter enterocytes at the apical side, as *L. innocua* expressing internalin can infect enterocytes and is detected just beneath microvilli (9).

The tropism of *Listeria* internalin for enterocytes differs from that of *Yersinia* inva-

sin, which targets apically expressed β 1-integrins in M cells and permits translocation of *Yersinia* through these cells (19, 20). The internalin E-cadherin interaction is thus a potential tool for specific drug targeting to enterocytes and delivery across the intestinal barrier. In humans, *L. monocytogenes* can also cross the fetoplacental and the blood-brain barriers, which contain E-cadherin-expressing cells (21–23). Whether internalin is involved in these other steps of the infection is unknown. Interestingly, cytomegalovirus and *Toxoplasma gondii* have the same double tropism for the maternofetal unit and the brainstem.

Transgenic mice have been instrumental for studying the molecular mechanisms of viral infections, including poliomyelitis [mice expressing human poliovirus receptor (24)] and measles [mice expressing human CD46 (25)]. As shown here, transgenic mice can also provide models for human bacterial diseases.

References and Notes

1. B. Lorber, *Clin. Infect. Dis.* **24**, 1 (1996).
2. C. B. Dalton et al., *N. Engl. J. Med.* **336**, 100 (1997).
3. P. Aureli et al., *N. Engl. J. Med.* **342**, 1236 (2000).
4. J. L. Gaillard, P. Berche, C. Frehel, E. Gouin, P. Cossart, *Cell* **65**, 1127 (1991).
5. J. Mengaud, H. Ohayon, P. Gounon, R. M. Mège, P. Cossart, *Cell* **84**, 923 (1996).
6. A. S. Yap, W. M. Brieher, B. M. Gumbiner, *Annu. Rev. Cell Dev. Biol.* **13**, 119 (1997).
7. M. Lecuit et al., *EMBO J.* **18**, 3956 (1999).

8. P. Racz, K. Tenner, E. M  r , *Lab. Invest.* **26**, 694 (1972).
9. Supplementary data and information on experimental protocols are available on Science Online at www.sciencemag.org/cgi/content/full/292/5522/1722/DC1.
10. M. Lecuit and P. Cossart, unpublished data.
11. The $-1178 +28$ rat *iFABP* promoter sequence was amplified and subcloned in-frame and upstream of *hEcad* cDNA in pSK-(hEcad) (7). The human β -globin intron 2 and a polyadenylate tract was placed downstream of *hEcad* to improve transcriptional efficiency in transgenic mice. The purified 5545–base pair DNA construct was microinjected in (C57BL/6J \times SJLJ) F_2 zygotes and reimplanted in pseudopregnant (C57BL/6J \times CBA/J) F_1 mice (9).
12. M. L. Hermiston, M. H. Wong, J. I. Gordon, *Genes Dev.* **10**, 985 (1996).
13. B. Pron et al., *Infect. Immun.* **66**, 747 (1998).
14. P. Cossart, M. Lecuit, *EMBO J.* **17**, 3797 (1998).
15. T. M. Mayhew, R. Myklebust, A. Whybrow, R. Jenkins, *Histol. Histopathol.* **14**, 257 (1999).
16. S. Dramsi et al., *Mol. Microbiol.* **16**, 251 (1995).
17. Y. Shen, M. Naujokas, M. Park, K. Ireton, *Cell* **103**, 501 (2000).
18. C. Birchmeier, E. Gherardi, *Trends Cell Biol.* **8**, 404 (1998).
19. A. Marra, R. R. Isberg, *Infect. Immun.* **65**, 3412 (1997).
20. R. Schulte et al., *Cell. Microbiol.* **2**, 173 (2000).
21. D. Figarella-Branger et al., *Acta Neuropathol.* **89**, 248 (1995).
22. L. L. Rubin et al., *J. Cell Biol.* **115**, 1725 (1991).
23. Y. Shimoyama et al., *Cancer Res.* **49**, 2128 (1989).
24. R. B. Ren, F. Constantini, E. J. Gorgacz, J. J. Lee, V. R. Racaniello, *Cell* **63**, 353 (1990).
25. M. B. A. Oldstone et al., *Cell* **98**, 629 (1999).
26. We thank M. Takeichi for the gift of HECD1 hybridoma; J. I. Gordon for rat *iFABP* promoter DNA; V. R. Racaniello for human β -globin intron 2 DNA; H. Khun for the immunolabeling of tissue sections; and S. Dramsi, G. Milon, and H. Ohayon for help in preliminary experiments. These studies were supported by Association de Recherche sur le Cancer, the European Economic Commission, Minist re de l'Education Nationale, de l'Enseignement Sup rieur et de la Recherche, CNRS, and Institut Pasteur. P.C. is an international investigator from the Howard Hughes Medical Institute.

14 February 2001; accepted 24 April 2001

Structure of Complement Receptor 2 in Complex with Its C3d Ligand

Gerda Szakonyi,^{1*} Joel M. Guthridge,^{2*} Dawei Li,¹ Kendra Young,² V. Michael Holers,² Xiaojiang S. Chen^{1†}

Complement receptor 2 (CR2/CD21) is an important receptor that amplifies B lymphocyte activation by bridging the innate and adaptive immune systems. CR2 ligands include complement C3d and Epstein-Barr virus glycoprotein 350/220. We describe the x-ray structure of this CR2 domain in complex with C3d at 2.0 angstroms. The structure reveals extensive main chain interactions between C3d and only one short consensus repeat (SCR) of CR2 and substantial SCR side-side packing. These results provide a detailed understanding of receptor-ligand interactions in this protein family and reveal potential target sites for molecular drug design.

Complement receptor type 2 (CR2 or CD21), the receptor for complement component C3d, is a key interface between innate and adaptive immunity (1). C3d attaches to foreign antigens (such as invading microorganisms) (2) and these C3d-bound antigens amplify B cell responses by simultaneously binding to CR2 through C3d and to the B cell receptor (BCR) via the bound antigen (3). The cross-linking of CR2 to the BCR amplifies a signal transduction cascade through the CR2/CD19/CD81 co-activation complex (1). CR2 mediates the interaction of C3-bound HIV-1 as an immune complex with B cells and so promotes transfer of virus and infection of CD4 T cells (4). Human CR2 is also a receptor for CD23 (5) and is the obligate receptor for the Epstein-Barr virus (EBV) (6). In addition, CR2 is essential for the development of normal humoral immunity to T-dependent antigens (7–9) and has been implicated

in the maintenance of B cell self-tolerance and the development of autoimmunity (10).

Interactions with all three human CR2 ligands require the first two of 15 or 16 short

consensus repeats (SCR1 and SCR2) of CR2 (11, 12). SCR domains, like immunoglobulin domains, are found in many proteins from both complement and non-complement families and mediate diverse biological functions (13). SCR domains have a conserved core structure but variable orientations between domains mediated in part by relatively short three to eight amino acid inter-SCR linker peptides (14–16). At least two SCR domains are required to mediate protein-protein interaction, and the relative angle and orientation between domains is likely to contribute to biologic diversity and specificity. The lack of a high-resolution structure of a receptor-ligand complex in this family has hindered our understanding of the molecular recognition mechanisms of this class of proteins. To gain insight into CR2 interactions, we have determined the crystal structure of the CR2 SCR1 and SCR2 domain in complex with C3d at 2.0   (17).

The complex contains a V-shaped CR2 receptor binding to a globular C3d ligand (Fig. 1A and Table 1). The V-shaped CR2

Table 1. Structure determination and refinement. ASU, asymmetric unit; rmsd, root mean square deviation.

	Data collection statistics	
Space group		R32
Unit cell length (�)		$a = b = 170.5, c = 173.8$
Molecules/ASU		3
Resolution (�)		25.0–2.04
Completeness (last bin)		94.1 (83.6)
Total reflections		255801
Unique reflections		65612
R_{sym} (last bin)%*		6.7 (22.3)
I/σ (last bin)		10.8 (3.7)
	Refinement statistics	
% of reflections for R_{free}		10
R_{work}/R_{free}		20.8/23.9
Rmsd from ideality		
Bond length (�)		0.006
Bond angle (�)		1.10
Dihedral angle (�)		16.8
Ramachandran plot (core, disallowed)		92.3 (0)
Average B factor		33.98
Rmsd of B factor (� ²)		1.2
Protein atoms in the model		8878
H ₂ O in the model		580

* $R_{sym} = \sum_j |I(j) - \langle I(j) \rangle| / \sum_j I(j)$, where $I(j)$ is the i th measurement of reflection j , and $\langle I(j) \rangle$ is the overall weighted mean of j measurements.

¹Department of Biochemistry and Molecular Genetics, ²Departments of Medicine and Immunology, University of Colorado Health Science Center, School of Medicine, Denver, CO 80262, USA.

*These authors contributed equally to this work.

†To whom correspondence should be addressed. E-mail: Xiaojiang.Chen@uchsc.edu